



Duan Qingyun (Orcid ID: 0000-0001-9955-1512)

Pan Yun (Orcid ID: 0000-0001-9634-7612)

Gong Wei (Orcid ID: 0000-0003-3622-7090)

Di Zhenhua (Orcid ID: 0000-0003-0188-0479)

Lei Xiaohui (Orcid ID: 0000-0002-6749-6114)

Zheng Longqun (Orcid ID: 0000-0001-9929-443X)

The effectiveness of the South-to-North Water Diversion Middle Route Project on water delivery and groundwater recovery in North China Plain

Chong Zhang^{a,b}, Qingyun Duan^{c,d}, Pat J.-F. Yeh^e, Yun Pan^{f,g}, Huili Gong^{f,g}, Wei Gong^{a,b}, Zhenhua Di^{a,b}, Xiaohui Lei^h, Weihong Liao^h, Zhiyong Huangⁱ, Longqun Zheng^{f,g}, Xueru Guo^j

^aInstitute of Land Surface System and Sustainable Development, Beijing Normal University, Beijing, China

^bState Key Laboratory of Earth Surface Processes and Resource Ecology, Beijing Normal University, Beijing, China

^cState Key Laboratory of Hydrology-Water Resources and Hydraulic Engineering, Hohai University, Nanjing, China

^dCollege of Hydrology and Water Resources, Hohai University, Nanjing, China

^eDiscipline of Civil Engineering, Monash University (Malaysia Campus), Malaysia

^fBeijing Laboratory of Water Resources Security, Capital Normal University, Beijing, China

^gCollege of Resource Environment and Tourism, Capital Normal University, Beijing, China

This article has been accepted for publication and undergone full peer review but has not been through the copyediting, typesetting, pagination and proofreading process which may lead to differences between this version and the Version of Record. Please cite this article as doi: 10.1029/2019WR026759

^hState Key Laboratory of Stimulation and Regulation of Water Cycle in River Basin, China
Institute of Water Resources and Hydropower Research, Beijing, China

ⁱDepartment of Earth Sciences, The University of Hong Kong, Hong Kong, China

^jDepartment of Statistics, Beijing Normal University, Beijing, China

Corresponding author:

Qingyun Duan, State Key Laboratory of Hydrology-Water Resources and Hydraulic Engineering, Hohai University, Nanjing, China, qyduan@hhu.edu.cn

Key Points:

- MRP is shown to be effective in meeting water delivery target in North China Plain
- MRP contributes to the recovery of groundwater level in North China Plain
- Sensitivity of MRP effectiveness in water delivery and groundwater recovery is examined

Abstract

The South-to-North Water Diversion Middle Route Project (MRP), which started its operation in December 2014, was designed to transfer water from Danjiangkou Reservoir (DR) in Hanjiang River Basin to North China Plain (NCP) to alleviate water shortage and long-term groundwater depletion in the water-receiving region. This study investigates the effectiveness of actual MRP operation during 2015-2018 using the observed water budget data collected from DR and the groundwater level data from 559 monitoring wells. Assuming that MRP was in operation during 2005-2014, ensemble water diversion simulations were performed to study the sensitivity of MRP effectiveness to two important factors: the downstream water demand of DR (D_{wd}) and the ratio (I_r) of water diversion volume (Q_d) replacing groundwater pumping in NCP. Even though the observed and simulated mean annual Q_d during 2015-2018 (i.e., 4.3 km³/yr and 7.0 km³/yr, respectively) failed to meet the original water delivery target of 9.5 km³/yr due to its short operation and the coincidence with a dry cycle, MRP is effective in groundwater recovery as an increasing trend (+0.3 km³/yr) in groundwater storage (GWS) was observed in NCP during 2015-2018. MRP's effectiveness is sensitive to D_{wd} and I_r . D_{wd} should not exceed 23.0 km³/yr to guarantee Q_d reaching the original target, and I_r should not be less than 33% to guarantee GWS recovery. Those findings suggest that a reasonable decrease of D_{wd} and an increase of I_r are the recommended pathway to ensure the effectiveness of MRP in meeting both water delivery and groundwater recovery targets.

1. Introduction

Uneven spatio-temporal distribution of water resources has led to water scarcity in many densely populated regions in the world (Pokhrel et al., 2016; Wada et al., 2016). In China, half of the population and two-thirds of farmlands are located north of the Qinling-Huaihe demarcation line where water resources are only one-fifths of the national total (Liu and Du, 1985; Liu and Zheng, 2002). Annual available water resources per capita in Northern China ($\sim 910 \text{ m}^3/\text{yr}$) are far less than in Southern China ($\sim 3180 \text{ m}^3/\text{yr}$) (Ministry of Water Resources in China, 2018), and also below the recommended global baseline for water stress ($1700 \text{ m}^3/\text{yr}$) (Falkenmark and Widstrand, 1992). Problems due to water scarcity in Northern China have become increasingly severe with rapidly expanding agriculture and urbanization over the last several decades (Cai, 2008; Crow-Miller et al., 2017; Gong et al., 2018; Liu and Xia, 2004; Rogers et al., 2016).

The South-to-North Water Diversion Project has been constructed to reallocate water resources in China (Liu and Du, 1985; Liu and Zheng, 2002). The Middle Route Project (MRP), one of the three water diversion routes (eastern, middle and western) under the South-to-North Water Diversion Project, was designed to transfer water from the Danjiangkou Reservoir (DR) in the southern part of Hanjiang River Basin (HRB) to the water-scarce North China Plain (NCP) (Figure 1a). The hydroclimatic condition and water management practices differ considerably between two regions. Precipitation shows a distinct north-to-south upward gradient, with annual mean of 545.0 and 956.1 mm/yr for NCP and HRB, respectively (Figure 1b). Annual total water demands with the amount of 34.2 and 13.5 km³ in NCP and HRB, respectively, are supplied jointly by surface water and groundwater at different ratios (HRWCC, 2018; YRWCC, 2018) (Figure 1c). The surface water/groundwater supply ratios are 34%/63% and 87%/13% in NCP and HRB, respectively, with the remaining small percentages in NCP supplied by recycled water (Figure 1c). The groundwater level in NCP has dropped continually at a rate of 0.5~2.0 m/yr over the past 60 years (Gong et al., 2018; Huang et al., 2015; Pan et al., 2017). Long-term groundwater depletion has inevitably resulted in a range of adverse environmental problems such as land subsidence, seawater intrusion, a reduction of river flow, and adverse ecological impacts (Gong et al., 2018; Li et al., 2017; Shang et al., 2016).

Reversing the declining trend of groundwater level in NCP is one of the major objectives of MRP water diversion (Liu and Xia, 2004; Liu and Zheng, 2002). According to the Office of South-to-North Water Diversion Project Construction Committee (OSNPCC,

<http://nsbd.mwr.gov.cn/>), the DR dam was heightened from 162 m to 176.6 m during 2005-2010 to meet the water supply requirement of MRP. Consequently, the normal reservoir water level (RWL) of DR was elevated from 157 m to 170 m, and the storage capacity was increased from 17.5 km³ to 29.1 km³ (Li et al., 2017; Liu et al., 2012). The designed water diversion rate of MRP is 9.5 km³/yr (OSNPCC, 2016), which is the planned total volume of water that would be transferred annually once MRP is fully operational. Since the start of its operation in December 2014, a total of 17.0 km³ water has been delivered to NCP (i.e., 2.3, 3.6, 4.8 and 6.3 km³/yr in 2015 to 2018 respectively). The delivered volume is below the target of 9.5 km³/yr, mainly due to the incompleteness of certain ancillary delivery channels and facilities (Lei et al., 2018; Ma et al., 2016). The MRP-delivered water, except for partly compensating environmental flow, replenishing reservoirs, and recharging aquifers, was mainly used to replace the domestic and industrial consumption originally supplied by groundwater in NCP (Yang et al., 2012; Yang et al., 2018). Since then, the recovery of groundwater level has been reported in some locations. For example, a recovery of 9 m from 2014 to 2017 was observed in the Huairou Waterworks in Beijing (He et al., 2019; Long et al., 2020; Rogers et al., 2019; Wang et al., 2019).

Even with the commencement of the MRP operation, two issues related to the MRP implementation are still being debated. The first is whether DR can meet the designed water delivery target without affecting downstream water supply (Stone and Jia, 2006). Previous studies investigated the dominant factors affecting water diversion, including the inflow to DR (Chen et al., 2007; Liu et al., 2012; She et al., 2017; Sun et al., 2014), downstream water demand (Li et al., 2015; Li et al., 2017; Wang et al., 2015; Xu and Chang, 2009), and DR operation (Song et al., 2018; Wang et al., 2014; Wang et al., 2016; Yang et al., 2017; Zhou and Guo, 2013). The inflow to DR has large inter-annual variability, ranging from 17.1 to 79.5 km³/yr during the period 1960-2013 (Liu et al., 2012; She et al., 2017), while the downstream water demands estimated by the ecohydrological models are relatively stable ranging from 12.2 to 16.2 km³/yr (Li et al., 2015; Li et al., 2017; Xu and Chang, 2009). If the operational principle were enforced that DR inflow must guarantee downstream water demand, there would not have been enough water to be diverted during dry years (Liu et al., 2012, 2015; Liu et al., 2018; She et al., 2017), which would pose a serious challenge to the effectiveness of MRP in delivering water (Liu et al., 2015; She et al., 2017).

The second issue is whether the delivered water from MRP can help recover the declining

groundwater level in NCP. Most previous studies that investigated the influences of MRP on aquifer storage recovery were mainly based on model simulations (e.g., Cao et al., 2013; Li et al., 2017; Xia et al., 2018; Yang et al., 2012; Ye et al., 2014; Zhang et al., 2018). These studies commonly set a constant water diversion rate throughout the study period and assumed that the MRP-delivered water can be used to reduce groundwater pumping. For example, 1.0 km³/yr to the Beijing plain for 2009-2019 (Yang et al., 2012), 6.0 km³/yr to the NCP for 2015-2030 (Cao et al., 2013), and 6.5 km³/yr to the Haihe River basin for 1999-2005 (Ye et al., 2014). Their general findings were that the implementation of MRP could partially help the groundwater level recovery in small local regions only, but unable to reverse the large-scale groundwater depletion (Cao et al., 2013; Li et al., 2017; Yang et al., 2012; Ye et al., 2014). More strict restriction on groundwater pumping (e.g., shutdown private wells) and more highly-efficient utilization of water resources (e.g., develop water-saving agriculture) will be required to alleviate groundwater shortage (Lei et al., 2018; Rogers et al., 2019; Xia et al., 2018; Yang et al., 2018).

Although the aforementioned studies have attempted to explore different specific issues of MRP, few or no studies have provided a holistic analysis on the effectiveness of MRP in both water delivery and groundwater recovery. It is noteworthy to emphasize that MRP operation is a dynamic process connecting the water cycle between NCP and HRB (Lei et al., 2018; Liu and Zheng, 2002; Wang et al., 2016). The assessment of MRP effectiveness in delivering water needs to consider the constraints imposed both by dynamic DR operation and by downstream water demand in HRB (e.g., Li et al., 2017; Wang et al., 2014; Wang et al., 2015). Additionally, the actual MRP water diversion rate in the operational period (2015 till now) is time-varying, implying that the use of constant water diversion rate in previous modelling studies was not realistic (e.g., Cao et al., 2013; Li et al., 2017; Yang et al., 2012; Ye et al., 2014; Xia et al., 2018; Zhang et al., 2018). Model simulation may reveal significant insights regarding the influences of MRP on groundwater recovery, but is unable to reflect the actual groundwater recovery in NCP.

In this study, a dynamic water diversion model is developed to simulate the water diversion from the DR in HRB to the NCP. Based on the available practical information, model simulation and the water budget data collected from DR during the 2015-2018 actual operation period of MRP, the effectiveness of MRP in delivering water is evaluated. Moreover, the 2005-2018 monthly measurements of groundwater level data from a total of 559 monitoring wells in

NCP are used to explore the effectiveness of MRP in recovering groundwater. Assuming that MRP was in operation during 2005-2014, ensemble water diversion simulations were performed to investigate the sensitivity of MRP effectiveness (both in water delivery and groundwater recovery) to two important uncertain factors: the downstream water demand of DR in HRB and the ratio of water diversion volume replacing groundwater pumping in NCP. The results obtained in this study should be of high significance in assessing the MRP effectiveness and guiding the management of MRP in the future.

2. Materials and Methods

2.1. Dynamic Water Diversion Model

The MRP originates from DR in HRB and delivers water through a canal to NCP. The water budget equation for DR can be written as follows:

$$\Delta RWS = Q_{in} - Q_{out} - Q_d \quad (1)$$

where ΔRWS [L^3/T] is the reservoir water storage change; Q_{in} [L^3/T] and Q_{out} [L^3/T] are the DR inflow and outflow, respectively; and Q_d [L^3/T] is the water diversion volume. The total release from DR, $Q_{out} + Q_d$, needs to meet the water demand from downstream of DR (D_{wd} [L^3/T]), and the water delivery target Q_d , through an operational rule explained below.

Figure 2a displays the operational rule of DR as provided by OSNPCC (Yang et al., 2017). Five water diversion rates (i.e., 420, 350, 300, 260 and 135 m^3/s) can be made according to four operational curves (e.g., Curve-1 to Curve-4) corresponding to four different RWL heights at the beginning of the year, with each month divided into three 10-day operation periods. Based on the operational curves (Figure 2a), RWL should be controlled within the range between 145~170 m. For flood control purpose, RWL cannot exceed 160 m from mid-June to mid-August and 163.5 m from late-August to early-October. The water diversion rate can reach the maximum of 420 m^3/s if RWL is in the pink zone (Figure 2a). If the RWL falls in the grey zone (i.e., the zone between the Curve-1 and Curve-2), the water diversion rate is set to be 350 m^3/s . Similarly, the diversion rate is 300 m^3/s when RWL falls in the blue zone, 260 m^3/s in the green zone, and 135 m^3/s in the orange zone. The water diversion is stopped when RWL falls below the baseline at 145 m.

Following the operational principle set by MRP, a dynamic water diversion model is developed to parameterize the aforementioned reservoir operation process. The model runs at the 10-day

time step, consistent with the interval of the MRP operations. The simulation algorithm is summarized as follows:

Step-1: Set the initial RWS to the volume at the start of actual MRP operation. Then check whether Q_{in} is higher than D_{wd} . If yes, release a fraction of Q_{in} equal to D_{wd} as Q_{out} and impound the remainder, $Q_{in}-Q_{out}$, to increase RWS. If not, reduce RWS by $Q_{out}=D_{wd}-Q_{in}$.

Step-2: Convert RWS into RWL using the DR rating curve (Figure 2b). Determine the water diversion rate based on the DR operational rules (Figure 2a).

Step-3: Compute Q_d by multiplying the water diversion rate with time interval. Update RWS by deducting Q_d from RWS.

Note that, in Step-1, the initial RWS is only valid in the first time step and can be replaced by the updated RWS from Step-3. If the updated RWS is not full and Q_{in} is higher than D_{wd} , Q_{out} is equal to D_{wd} and RWS can then be replenished by the surplus amount from Q_{in} (i.e., $Q_{in}-D_{wd}$). Still, RWS is not allowed to exceed normal storage capacity (29.1 km^3) during the non-flooding period (October-April) even if a large Q_{in} surplus occurs. During the flooding period (May-September), if the RWL falls in the flood control zone (Figure 2a), the model can simulate the flood-control processes by keeping RWL below the flood-control level in the early stage, and then begin to store water in the later stage. A portion of water has to be abandoned in this period in order to provide adequate storage capacity for flood prevention (Li et al., 2017; Wang et al., 2014; Yang et al., 2016, 2017). In this case, Q_{out} is larger than D_{wd} . Additionally, if RWL falls below the baseline water level of 145 m, DR stores all Q_{in} to increase RWS instead of releasing water to meet D_{wd} and Q_d , in which case, Q_{out} is less than D_{wd} (Figure 2a).

The water diversion (Q_d) is delivered along the MRP canal mainly by gravity force to NCP (Figure 1a). A small fraction of Q_d is lost by channel evaporation, but it is compensated by precipitation and influent into the channels (Ma et al., 2016). Therefore, it can be reasonably assumed that the Q_d from DR is approximately equal to the total water received in NCP (e.g., Li et al., 2017; Yang et al., 2012). Although Q_d in NCP has many users (e.g., compensating environmental flow and replenishment of reservoirs), the replacement of Q_d to groundwater pumping (Q_p) is the most direct and effective way to promote the recovery of groundwater storage (GWS) in NCP. Hence the corresponding ratio (I_r) of Q_d replacing Q_p is identified as the key factor to control the extent of the GWS recovery in this study.

GWS variations in NCP are actually the results of the interactions of multiple recharge sources (e.g., precipitation infiltration and irrigation return flow) and discharge terms (e.g., Q_p and baseflow) in groundwater budget (Cao et al., 2013). Since the natural discharge from aquifers (i.e., baseflow) in NCP is nearly negligible due to the progressively deeper groundwater level depth (Cao et al., 2013; Kendy et al., 2004), the decrease of Q_p does not increase the natural aquifer discharge in the short term, nor does it affect the recharge terms of groundwater budget. Thus, for the entire NCP, it is reasonable to assume that the reduction of Q_p is equal to the increase of GWS at regional scale. The simulated Q_d , after a discount by I_r , is gradually accumulated at the observed GWS baseline during the study period (see Section 2.3) to simulate the recovery of groundwater in NCP. Although the groundwater simulation designed here is only based on the simple groundwater budget without incorporating the spatio-temporal variations of precipitation infiltration and natural discharge, it can be taken as a direct and effective method to explore the effectiveness of MRP in recovering groundwater throughout the entire NCP.

2.2. Data Sources

Two data sets, including Q_{in} and D_{wd} of DR, are used to drive the dynamic water diversion simulations in HRB. The 2005-2018 daily time series of Q_{in} , Q_{out} , RWS and RWL data of DR were collected from the official reservoir management system of the Hydrological Bureau in the Hubei province (<http://113.57.190.228:8001/web/Report/BigMSKReport#>), and were aggregated into the 10-day interval, consistent with the time unit of the DR operational rules (Figure 2a). Figure 3a shows the 10-day aggregated time series of Q_{in} , Q_{out} , and RWS of DR during 2005-2018. Figure 3b and 3c plot their corresponding mean annual cycles before (2005-2014) and after (2015-2018) the MRP implementation, respectively.

D_{wd} is estimated based on the 2015-2018 mean annual cycle of Q_{out} . As seen in Figure 3a, RWS increased sharply at the end of 2014 due to the fact that the dam-heightened DR impounded more Q_{in} to supply water for the MRP. The 2005-2014 and 2015-2018 mean annual cycles of Q_{out} follow closely that of Q_{in} (Figure 3b and 3c). Note that Q_{out} during 2005-2014 had peaks in June-September (Figure 3b), while during 2015-2018 its variability was milder except for the sharper peak in October due to the natural flood drainage occurred in late 2017 (Figure 3a and 3c). Q_{out} decreased during 2015-2018 due to Q_{in} reduction and RWS filling. Since the dispatching of DR had taken the protection of downstream environmental benefits into accounts and the cascade reservoirs constructed upon downstream river channel have positive

regulation of flow regime in HRB (Song et al., 2018; Yang et al., 2017; Zhou and Guo, 2013), it is reasonably suggested that the decrease of Q_{out} neither causes significant downstream water shortage nor degrades its environmental values, indicating that Q_{out} can meet D_{wd} in HRB throughout the entire MRP operation period. Considering that annual D_{wd} pattern changes little in the short term, it is reasonable to assume that the 2015-2018 mean annual cycle of Q_{out} (without considering the flood drainage in late 2017) is repeated as the D_{wd} in each year recently (Figure 3c). The estimated annual mean D_{wd} is $23.2 \text{ km}^3/\text{yr}$, which is larger than the reported $12.2\sim 16.2 \text{ km}^3/\text{yr}$ in literatures (Li et al., 2015; Li et al., 2017; Wang et al., 2015; Xu and Chang, 2009) and hence implies the higher reliability to meet downstream water utilization.

The data of 2005-2018 monthly groundwater level measurements from 559 unconfined wells in NCP were collected from annual groundwater yearbook published by the Institute of China Geological Environment Monitoring (ICGEM, 2018). Figure 4a plots the spatial distribution of well positions. The wells are relatively uniformly located over the NCP region. Each well follows a strict quality control that the groundwater level data records have at least 60% of temporal coverage during the study period. The GWS data were then calculated by multiplying each well-observed groundwater level with the specific yield ($0.025\sim 0.290$) referenced from Zhang et al. (2009).

Since no explicit I_r value was recorded during 2015-2018, the 2015-2018 annual Q_d data and the 2005-2018 annual Q_p data collected from the official water resources bulletins annually published by Chinese government (HRWCC, 2018), are used to evaluate the value of I_r in this study. As seen in Figure 4b, annual Q_p was decreased at a rate of $-0.4 \text{ km}^3/\text{yr}$ during 2005-2014, and accelerated to $-1.0 \text{ km}^3/\text{yr}$ during 2015-2018. Assuming that annual Q_p during 2015-2018 would still decrease by $-0.4 \text{ km}^3/\text{yr}$, it is reasonably speculated that the accelerated reduction of Q_p is due to the replacement of Q_p by Q_d . Hence the annual total of excess reduction of Q_p (6.8 km^3) during 2015-2018 can be mainly attributed to the water replacement from Q_d (17.0 km^3). The corresponding I_r value is therefore equal to 40%. This value is used to represent the most realistic case in ensemble water diversion simulations and also used as an initial value in the following sensitivity test of MRP effectiveness in groundwater recovery.

2.3. Design of Sensitivity Test

To test the sensitivity of MRP effectiveness both in water delivery and groundwater recovery, ensemble water diversion simulations are designed by varying D_{wd} and I_r since Q_d in HRB is

largely controlled by D_{wd} and GWS recovery in NCP is highly dependent on I_r (Li et al., 2017; Wang et al., 2015). Specifically, fifty sets of D_{wd} with the equal-interval scaling within $\pm 50\%$ (i.e., annual D_{wd} changes within 11.6~34.8 km³/yr) and fifty values of I_r with the equal-interval sampling within $\pm 50\%$ (i.e., I_r changes within 20~60%) are considered in ensemble simulations. Given that the actual operation period of MRP (2015-2018) is relatively short, ensemble water diversion simulations are performed by assuming that MRP was in operation during 2005-2014. Among them, the case that $D_{wd}=23.2$ km³/yr and $I_r=40\%$ is taken as the most realistic simulation of MRP operation. Other simulations represent the estimated sensitivity of MRP effectiveness to varying D_{wd} and I_r .

3. Results and Discussion

3.1. MRP Effectiveness in Delivering Water

Figure 5 plots the simulated monthly variations of water budget components of DR (RWS, Q_{in} , Q_{out} and Q_d) during 2015-2018, which were compared with the observed data in the actual operation period of DR. The temporal variations of RWS from simulation and observation agree well with each other (Figure 5a). However, since the simulated results represent the case of full operation and the observed ones represent the case of trial operation for DR, RWS from simulation fluctuates more than that from observation and both of them reach the higher levels with large Q_{in} replenishment (Figure 5a). The simulated Q_{out} varies smoothly compared with the observed Q_{out} (Figure 5b). The most notable case is the reduction of Q_{out} from 11.5 km³ to 3.1 km³ in October 2017, which is mainly due to that the DR under full operation consumes more RWS and empties more storage in non-flooding periods, and then impounds more Q_{in} to decrease Q_{out} in flooding periods (Figures 5a and 5b) (Yang et al., 2016, 2017). Following the DR operational rules, high Q_d is supported by high RWS (Figure 5c). Q_d peaks in June-September, corresponding to the peak periods of RWS and Q_{in} (Chen et al., 2007; Liu et al., 2012; She et al., 2017). However, both Q_d and RWS tend to be low when Q_{in} is in deficiency. The most notable case is the deficiency of Q_d around 2016, corresponding to two-year consecutive shortage of Q_{in} . The increased Q_d during 2017-2018 implies that Q_d deficiency can be quickly improved after RWS receives a huge Q_{in} replenishment (Figures 5a and 5c).

MRP effectiveness in delivering water can be interpreted by comparing the observed and simulated annual Q_d with the designed water delivery target (9.5 km³/yr) during 2015-2018, as shown in Figure 5d. The mean annual Q_d from observation is only 4.3 km³/yr, failing to meet

the designed water delivery target ($9.5 \text{ km}^3/\text{yr}$). The mean annual Q_d from simulation is $7.0 \text{ km}^3/\text{yr}$, significantly larger than observation, but still smaller than the designed target. Except for the subjective reason that MRP is not in full operation (Ma et al., 2016; Lei et al., 2018), one compounding reason is that three out of four years during the 2015-2018 actual MRP operation period are dry years with significant Q_{in} shortage (Liu et al., 2015; Liu et al., 2018). The mean annual Q_{in} during 2015-2018 is only $27.0 \text{ km}^3/\text{yr}$ (Figure 5d), 9.4 and $9.1 \text{ km}^3/\text{yr}$ less than that during 2005-2014 ($36.4 \text{ km}^3/\text{yr}$) and the 1960-2013 long-term mean level ($36.1 \text{ km}^3/\text{yr}$), respectively (Liu et al., 2012; She et al., 2017). The annual Q_{in} deficiency approximating the designed water delivery target is responsible for the Q_d deficiency. Annual Q_{in} varies between $19.5\sim 40.7 \text{ km}^3/\text{yr}$ during 2015-2018, and annual Q_d correspondingly varies between $3.3\sim 9.5 \text{ km}^3/\text{yr}$. These suggest that an elastic annual water diversion plan, rather than a fixed value, should be better in the MRP operation (Liu et al., 2012; She et al., 2017). Historically, Q_{in} has large interannual fluctuation ranging $17.1\sim 79.5 \text{ km}^3/\text{yr}$ (Liu et al., 2012; She et al., 2017), it is thus credible that Q_d can be significantly improved when Q_{in} turns to a wet trend.

3.2. MRP Effectiveness in Recovering Groundwater

To illustrate the variations of GWS before and after MRP implementation in NCP, we calculated the annual trends of GWS in each well during 2005-2014 and 2015-2018, and their corresponding spatial distributions are shown in Figures 6a and 6b, respectively. For the observations of 559 wells during 2005-2014 (Figure 6a), GWS showed a decreasing trend in 376 (67%) wells, whereas the rest 183 (33%) wells showed an increasing trend. During 2015-2018 (Figure 6b), however, GWS showed a decreasing trend in only 271 (48%) wells, whereas the rest 288 (52%) wells showed an increasing trend. Some wells observed the GWS recovery during 2005-2014 (e.g., in Cangzhou city, Figure 6a), which was related to the success of localized groundwater management (Shang et al., 2016). A majority of wells in Beijing city observed the GWS recovery during 2015-2018 (Figure 6b), which was attributed to the reduction of Q_p jointly caused by the replacement of Q_d and the steady increase of recycled water use (He et al., 2019; Long et al., 2020; Rogers et al., 2019; Wang et al., 2019). Figure 6c shows the 2005-2018 monthly time series of GWS variations in NCP. As seen, GWS during 2005-2014 showed a decreasing trend with a rate of $-2.2 \text{ km}^3/\text{yr}$, whereas that during 2015-2018 showed a slightly increasing trend with a rate of $+0.3 \text{ km}^3/\text{yr}$ (Figure 6c). The reversal trend was attributed to the further reduction of Q_p accelerated by Q_d replacement (Figure 4b).

The finding suggests that MRP water diversion is effective to a certain extent in recovering groundwater and GWS in NCP has begun to transition from depletion to localized recovery in specific areas.

Similar with previous studies (Cao et al., 2013; Yang et al., 2012; Ye et al., 2014), our results support that Q_d can result in GWS recovery in NCP. However, the observed areas and magnitudes of GWS recovery differ with those in previous modelling studies. The divergence between this study and previous ones can be attributed to the difference of hydroclimatic context based on the selection of different study periods. Except for the known factors that GWS responds differently to varying precipitation/irrigation infiltration and natural aquifer discharge (Kendy et al., 2004), the variations of groundwater exploitation in different periods likewise play a key role in determining the amounts of Q_d required for recovering GWS in NCP (Cao et al., 2013; Gong et al., 2018). Previous studies have found that GWS in NCP was drastically depleted in 1990s (Cao et al., 2013; Ye et al., 2014), resulting in frequent land subsidence and ecological environment deterioration (Li et al., 2017; Gong et al., 2018; Shang et al., 2016). Since the beginning of 21st century, problems caused by groundwater overexploitation have attracted widespread attention, and several water-saving measures have been proposed to reduce Q_p for the purpose of mitigating groundwater depletion (Cao et al., 2013; Liu and Zheng, 2002). By comparison, the decreasing trend of GWS in NCP was nearly $-7.0 \text{ km}^3/\text{yr}$ in 1990s (Cao et al., 2013; Gong et al., 2018), more than triple the trend in 2005-2014 at $-2.2 \text{ km}^3/\text{yr}$ (Figure 6c). Hence selecting 1990s as a simulation period in previous studies inevitably requires more Q_d to reverse the huge decreasing trend of GWS. In this study, the 2005-2018 observation of GWS variations exactly covers the periods before and after MRP implementation, meaning that the decreasing trend of GWS from well observations is more representative for evaluating the effectiveness of MRP in recovering groundwater.

3.3. Sensitivity of MRP Effectiveness to Varying D_{wd} and I_r

To study the sensitivity of MRP effectiveness in both water delivery and groundwater recovery, ensemble water diversion simulations with varying D_{wd} and I_r are performed during 2005-2014. Figures 7a and 7b depict the 2005-2014 monthly time series of Q_{in} and Q_d in DR with D_{wd} varying between $11.2\sim 34.8 \text{ km}^3/\text{yr}$, respectively. As seen, high Q_d is supported by the simultaneous occurrence of high Q_{in} and low D_{wd} (e.g., in 2005) (Liu et al., 2018). However, Q_d tends to be low when Q_{in} is in deficiency and D_{wd} increases gradually (Figures 7a and 7b). As the worst case where low Q_{in} and high D_{wd} occur simultaneously (e.g., in first half of 2014),

Q_d drops to zero accordingly (Figure 7b). This actually reflects the case in which an extreme drought challenges the MRP effectiveness in delivering water (Liu et al., 2002; Liu et al., 2015). It is noteworthy that a reported drought hit HRB between late 2010 and early 2011 (Liu et al., 2015), inducing the RWS of DR to drop below its dead storage level in May 2011 (Figure 3a). Our simulation suggests that the drought had impacts on Q_d with relatively large D_{wd} , but the impact strength was weaker than the case during 2008-2010 when Q_{in} experienced intermittent deficiency while D_{wd} increased during the flooding periods for consecutive years. The phenomenon implies that Q_d may be slightly sensitive to the short-term persistent drought, but can be seriously threatened by the long-term intermittent drought (Liu et al., 2012, 2015).

Figure 7c selectively plots the 2005-2014 monthly time series of the observed GWS and the simulated GWS variations after receiving the most realistic Q_d ($D_{wd}=23.2 \text{ km}^3/\text{yr}$, shown in Figure 7b) with varying I_r (40~60%) in NCP. As seen, the simulated GWS after receiving Q_d is always higher than the observed GWS without Q_d received. The decreasing GWS trend ($-2.2 \text{ km}^3/\text{yr}$) appears to have mitigation or reverse at varying degrees with the gradual accumulation of Q_d at monthly scale (Li et al., 2017; Xia et al., 2018; Ye et al., 2014; Zhang et al., 2018) (Figure 7c). The variations of I_r are directly associated with the degree of GWS mitigation or recovery. For the most realistic simulation where $D_{wd}=23.2 \text{ km}^3/\text{yr}$ ($Q_d=9.4 \text{ km}^3/\text{yr}$) and $I_r=40\%$, the simulated GWS recovers with an annual trend of $+1.8 \text{ km}^3/\text{yr}$ in NCP (Figure 7c). It is noteworthy that Q_d cannot offset the depletion of GWS in each year because both Q_d and GWS have their interannual variabilities (Figures 7b and 7c). In the case of concurrent drought occurring both in HRB and NCP (e.g., in 2014), the recovered GWS in previous water diversion would still be depleted inevitably (Liu et al., 2015). That is to say, if MRP runs stably, the recovery of GWS in NCP is likely to be intermittent and destined to take a long time.

The sensitivity of MRP effectiveness in delivering water can be interpreted by analyzing the simulated variations of 2005-2014 mean annual Q_d with varying D_{wd} . As shown in Figure 8a, a clearly negative correlation can be found between two mean annual values that an increase of $1.0 \text{ km}^3/\text{yr}$ in D_{wd} can decrease Q_d by $0.2 \text{ km}^3/\text{yr}$ (Figure 8a). As D_{wd} ranges $11.6\sim34.8 \text{ km}^3/\text{yr}$, Q_d varies between $6.6\sim11.6 \text{ km}^3/\text{yr}$ accordingly. It can be noted that D_{wd} cannot exceed $23.0 \text{ km}^3/\text{yr}$ to guarantee that the mean annual Q_d reaches the designed water delivery target ($9.5 \text{ km}^3/\text{yr}$). In the most realistic simulation where $D_{wd}=23.2 \text{ km}^3/\text{yr}$, DR delivers $9.4 \text{ km}^3/\text{yr}$ of Q_d that almost meets the designed water delivery target of MRP (Figure 8a). If referring to

the reported values of $D_{wd}=12.2\sim 16.2\text{ km}^3/\text{yr}$ in previous modelling studies (Li et al., 2015; Li et al., 2017; Wang et al., 2015; Xu and Chang, 2009), the mean annual Q_d can increase to $11.0\sim 11.5\text{ km}^3/\text{yr}$, completely meeting the designed target. These findings support that MRP is effective in meeting the designed water delivery target, but the effectiveness is sensitive to the variations of D_{wd} in HRB.

The sensitivity of MRP effectiveness in recovering groundwater is interpreted based on the results of ensemble water diversion simulations in Figure 8b, which plots the possible variations of annual GWS trends by varying both Q_d (D_{wd}) and I_r . The x-axis and y-axis represent mean annual Q_d and annual GWS trend, respectively. Different colors of band denote different I_r values ranging 20~60%. As seen in Figure 8b, the decreasing trend of GWS from observation ($-2.2\text{ km}^3/\text{yr}$ during 2005-2014) can always be mitigated or reversed in all ensemble simulations with Q_p replaced by Q_d . The results of most realistic simulation ($D_{wd}=23.2\text{ km}^3/\text{yr}$, $Q_d=9.4\text{ km}^3/\text{yr}$, and $I_r=40\%$) is marked by red star, corresponding to the increasing GWS trend of $+1.8\text{ km}^3/\text{yr}$. As for the worst case where $Q_d=6.6\text{ km}^3/\text{yr}$ (corresponding to $D_{wd}=34.8\text{ km}^3/\text{yr}$) and $I_r=20\%$, the decreasing GWS trend can be mitigated to a rate of $-0.9\text{ km}^3/\text{yr}$. If $I_r=33\%$, however, GWS can at least reach a new water equilibrium without further depletion in simulation. These indicate that using Q_d to replace Q_p (i.e., increasing I_r value) whenever possible is the recommended pathway to maximize the degree of GWS recovery. Given that D_{wd} controls Q_d in HRB and Q_d in turn controls GWS recovery in NCP, a hydrological teleconnection between HRB and NCP has been actually established since the start of actual MRP operation. That is to say, the magnitude of GWS recovery in NCP is remotely related to the variations of D_{wd} in HRB. The effectiveness of MRP in groundwater recovery is therefore sensitive to the variations of both I_r and D_{wd} .

4. Conclusion

MRP, which was designed to transfer water from DR in HRB to the water-scare NCP, has provoked many controversies since the start of its operation in December 2014. In this study, we first investigated the effectiveness of MRP in both the water delivery from DR and its influences on groundwater storage (GWS) recovery in NCP by using the collected observation data during 2015-2018 actual operation period of MRP. Ensemble water diversion simulations for the period of 2005-2014 were then performed by a dynamic water diversion model to study the sensitivity of MRP effectiveness to two important uncertain factors, namely, the downstream water demand of DR (D_{wd}) and the ratio (I_r) of water diversion volume (Q_d)

replacing groundwater pumping (Q_p) in NCP. The main conclusions of this study are as follows:

(1) During the actual MRP operation period (2015-2018), the values of mean annual Q_d from observation ($4.3 \text{ km}^3/\text{yr}$) and simulation ($7.0 \text{ km}^3/\text{yr}$) have not met the designed water delivery target ($9.5 \text{ km}^3/\text{yr}$). Except for the subjective reason that MRP was not in full operation, one compounding reason is that the inflow of DR in this period is seriously insufficient relative to long-term level. The simulated (observed) annual Q_d varies between $3.3\sim 9.5$ ($2.3\sim 6.3$) km^3/yr , implying that an elastic annual water diversion plan should be better in future MRP operation. The effectiveness of MRP in water delivery can be markedly improved when reservoir inflow turns to a wet trend.

(2) GWS in NCP has begun to recover with a rate of $+0.3 \text{ km}^3/\text{yr}$ during 2015-2018, which can be mainly attributed to the reduction of Q_p accelerated by Q_d replacement. The specific areas and magnitudes of GWS recovery differ between this study and previous ones. The major reason for this divergence is that previous studies generally conducted simulation during the period with relatively serious GWS depletion, and inevitably overestimated the amounts of water that need to be transferred from MRP. Our estimates are based on the observed data of groundwater level from 559 monitoring wells and the observation period can cover the actual MRP operation, indicating that the estimates are more representative for supporting the effectiveness of MRP in groundwater recovery.

(3) The effectiveness of MRP both in water delivery and groundwater recovery is sensitive to D_{wd} and I_r . An increase of $1.0 \text{ km}^3/\text{yr}$ in D_{wd} can decrease Q_d by $0.2 \text{ km}^3/\text{yr}$. To guarantee mean annual Q_d reaching the designed target ($9.5 \text{ km}^3/\text{yr}$), D_{wd} cannot exceed $23.0 \text{ km}^3/\text{yr}$. If considering that $D_{wd}=12.2\sim 16.2 \text{ km}^3/\text{yr}$, mean annual Q_d varies between $11.0\sim 11.5 \text{ km}^3/\text{yr}$, supporting that MRP is effective in water delivery. For GWS in NCP, I_r cannot be less than 33% in the worst case of $Q_d=6.6 \text{ km}^3/\text{yr}$ in order to guarantee GWS reaching a new water equilibrium (or recovery) without depletion. In the most realistic case where $Q_d=9.4 \text{ km}^3/\text{yr}$ and $I_r=40\%$, GWS recovers with a rate of $+1.8 \text{ km}^3/\text{yr}$. Given that a hydrological teleconnection between HRB and NCP has been established by MRP operation, the effectiveness of MRP in groundwater recovery is sensitive to the variations of both I_r and D_{wd} .

This study was performed in a short period of 2005-2018. The developed dynamic water diversion model is relatively simple, especially the module of regional groundwater budget

Accepted Article

estimation. The results from this study still need to be verified when more real operational data become available in the future. With the changing climate, future reservoir inflow and water demand in the MRP-connected regions might change, especially under warming scenarios. More specific studies by considering climate change effects on the effectiveness of MRP are needed in order to further adjust the MRP management in a timely manner.

Appendix:

Acronyms:	
DR	Danjiangkou Reservoir
D_{wd}	Downstream water demand
GWS	Groundwater storage
I_r	Ratio of Q_d replacing Q_p
MRP	The South-to-North Water Diversion Middle Route Project
NCP	North China Plain
Q_d	Water diversion volume
Q_{in}	Reservoir water inflow
Q_p	Groundwater pumping
Q_{out}	Reservoir water outflow
RWL	Reservoir water level
RWS	Reservoir water storage

Acknowledgments

This study was jointly supported by a research grant from Chinese Academy of Sciences Pioneer Exploration Project (No. XDA2006040104), National Basic Research Program of China (No. 2015CB953703), National Natural Science Foundation of China (No. 41771456) and China Scholarship Council (201906040156). The data of annual human water supply (use) in North China Plain and Hanjiang River Basin are collected from the official water resources bulletins respectively published by the Haihe River Water Conservancy Commission (<http://www.hwcc.gov.cn/hwcc/wwgj/xxgb/szygb/>) and the Yangtze River Water Conservancy Commission (<http://www.cjw.gov.cn/zwzc/bmgb/>). The water budget data of Danjiangkou Reservoir are available at the Hydrological Bureau of Hubei Province (<http://113.57.190.228:8001/web/Report/BigMSKReport#>). The data of groundwater level observation in North China Plain are excerpted from the annual groundwater yearbook published by the Institute of China Geological Environment Monitoring (<http://www.cigem.cgs.gov.cn/>). All these data are publicly available on the Data Sharing Repository of National Earth System Science Data Center (<https://www.doi.org/10.12041/geodata.10392011028646.ver1.db>). We thank the institutes who provided data for this study and the anonymous reviewers for their constructive comments.

References

- Cai, X. (2008). Water stress, water transfer and social equity in Northern China—Implications for policy reforms. *Journal of Environmental Management*, 87(1), 14–25. <https://doi.org/10.1016/j.jenvman.2006.12.046>
- Cao, G., Zheng, C., Scanlon, B. R., Liu, J., & Li, W. (2013). Use of flow modeling to assess sustainability of groundwater resources in the North China Plain. *Water Resources Research*, 49(1), 159–175. <https://doi.org/10.1029/2012WR011899>
- Chen, H., Guo, S., Xu, C., & Singh, V. P. (2007). Historical temporal trends of hydro-climatic variables and runoff response to climate variability and their relevance in water resource management in the Hanjiang basin. *Journal of Hydrology*, 344(3), 171–184. <https://doi.org/10.1016/j.jhydrol.2007.06.034>
- Crow-Miller, B., Webber, M., & Rogers, S. (2017). The Techno-Politics of Big Infrastructure and the Chinese Water Machine. *Water Alternatives*, 10(2), 233–249.
- Falkenmark, M., & Widstrand, C. (1992). Population and water resources: a delicate balance. *Population Bulletin*. Population Reference Bureau, Washington, DC.
- Gong, H., Pan, Y., Zheng, L., Li, X., Zhu, L., Zhang, C., Huang, Z., Li, Z., Wang, H., & Zhou, C. (2018). Long-term groundwater storage changes and land subsidence development in the North China Plain (1971–2015). *Hydrogeology Journal*, 26, 1417–1427. <https://doi.org/10.1007/s10040-018-1768-4>
- Haihe River Water Conservancy Commission (HRWCC) (2018). Annual Bulletin of Water Resources in Haihe River Basin. [Available at: <http://www.hwcc.gov.cn/>]
- He, Y., Li, S., Li, Y., Meng, X., & Liu, C. (2019). Effect of South-to-North water transfer project on recharge and water level in Chaobai River area [in Chinese]. *Beijing Water*, 3, 21–25.
- Huang, Z., Pan, Y., Gong, H., Yeh, P. J.-F., Li, X., Zhou, D., & Zhao, W. (2015). Subregional-scale groundwater depletion detected by GRACE for both shallow and deep aquifers in North China Plain. *Geophysical Research Letters*, 42. <https://doi.org/10.1002/2014GL062498>
- Institute of China Geological Environment Monitoring (ICGEM) (2018). China Geological Environment Monitoring: Annual Groundwater Yearbook [in Chinese], Vastplain House, Beijing.
- Kendy, E., Zhang, Y., Liu, C., Wang, J., & Steenhuis, T. S. (2004). Groundwater recharge from irrigated cropland in the North China Plain: Case study of Luancheng County, Hebei Province, 1949–2000. *Hydrological Processes*, 18(12), 2289–2302. <https://doi.org/10.1002/hyp.5529>
- Lei, X., Zheng, H., Shang, Y., & Wang, H. (2018). Assessing emergency regulation technology in the Middle Route of the South-to-North Water Diversion Project, China. *International Journal of Water Resources Development*, 34(3), 405–417. <https://doi.org/10.1080/07900627.2018.1441707>
- Li, L., Zhang, L., Xia, J., Gippel, C. J., Wang, R., & Zeng, S. (2015). Implications of Modelled Climate and Land Cover Changes on Runoff in the Middle Route of the South to North Water Transfer Project in China. *Water Resources Management*, 29, 2563–2579. <https://doi.org/10.1007/s11269-015-0957-3>

- Li, X., Ye, S., Wei, A., Zhou, P., & Wang, L. (2017). Modelling the response of shallow groundwater levels to combined climate and water-diversion scenarios in Beijing-Tianjin-Hebei Plain, China. *Hydrogeology Journal*, 25(6), 1733–1744. <https://doi.org/10.1007/s10040-017-1574-4>
- Li, Y., Cui, Q., Li, C., Wang, X., Cai, Y., Cui, G., & Yang, Z. (2017). An improved multi-objective optimization model for supporting reservoir operation of China's South-to-North water diversion project. *Science of the Total Environment*, 575, 970–981. <https://doi.org/10.1016/j.scitotenv.2018.05.124>
- Liu, C., & Du, W. (1985). Areal reallocation of China's water resources. *GeoJournal*, 10(2), 157–162.
- Liu, C., & Xia, J. (2004). Water problems and hydrological research in the Yellow river and the Huai and Hai river basins of China. *Hydrological Processes*, 18(12), 2197–2210. <https://doi.org/10.1002/hyp.5524>
- Liu, C., & Zheng, H. (2002). South-to-North water transfer schemes for China. *International Journal of Water Resources Development*, 18(3), 453–471. <https://doi.org/10.1080/0790062022000006934>
- Liu, H., Jie, Y., & Lian, F. (2018). The dynamic changes in the storage of the Danjiangkou reservoir and the influence of the South-North water transfer project. *Scientific Reports*, 8(1), 8710. <https://doi.org/10.1038/s41598-018-26788-5>
- Liu, X., Liu, C., Luo, Y., Zhang, M., & Xia, J. (2012). Dramatic decrease in streamflow from the headwater source in the central route of China's water diversion project: Climatic variation or human influence?. *Journal of Geophysical Research*, 117(D6), D06113. <https://doi.org/10.1029/2011JD016879>
- Liu, X., Luo, Y., Yang, T., Liang, K., Zhang, M., & Liu, C. (2015). Investigation of the probability of concurrent drought events between the water source and destination regions of China's water diversion project. *Geophysical Research Letters*, 42(20), 8424–8431. <https://doi.org/10.1002/2015GL065904>
- Long, D., Yang, W., Scanlon, B. R., Zhao, J., Liu, D., Burek, P., Pan, Y., You, L., & Wada, Y. (2020). South-to-North Water Diversion stabilizing Beijing's groundwater levels. *Nature Communications*, 11, 1–10. <https://doi.org/10.1038/s41467-020-17428-6>
- Ma, Y., Li, X., Wilson, M., Wu, X., Smith, A., & Wu, J. (2016). Water loss by evaporation from China's South-North water transfer project. *Ecological Engineering*, 95, 206–215. <https://doi.org/10.1016/j.ecoleng.2016.06.086>
- Ministry of Water Resources in China (2018). China Water Resources Bulletin. [Available at <http://www.mwr.gov.cn/sj/tjgb/szygb/>]
- Office of South-to-North Water Diversion Project Construction Committee (OSNPCC), State Council, PRC (2016). The South-to-North water diversion project. *Engineering*, 2(3), 262–386. <https://doi.org/10.1016/J.ENG.2016.03.022>
- Pan, Y., Zhang, C., Gong, H., Yeh, P. J.-F., Shen, Y., Guo, Y., Huang, Z., & Li, X. (2017). Detection of human-induced evapotranspiration using GRACE satellite observations in the Haihe River basin of China. *Geophysical Research Letters*, 44(1), 190–199. <https://doi.org/10.1002/2016GL071287>
- Pokhrel, Y., Hanasaki, N., Wada, Y., & Kim, H. (2016). Recent progresses in incorporating human land–water management into global land surface models toward their integration

- into Earth system models. *WIREs Water*, 3(4), 548–574. <https://doi.org/10.1002/wat2.1150>
- Rogers, S., Barnett, J., Webber, M., Finlayson, B., & Wang, M. (2016). Governmentality and the conduct of water: China's South-North Water Transfer Project. *Transactions of the Institute of British Geographers*, 41. <https://doi.org/10.1111/tran.12141>
- Rogers, S., Chen, D., Jiang, H., Rutherford, I., Wang, M., Webber, M., Crow-Miller, B., Barnett, J., Finlayson, B., Jiang, M., Shi, C., & Zhang, W. (2019). An integrated assessment of China's South–North water transfer project. *Geographical Research*, 58, 49–63. <https://doi.org/10.1111/1745-5871.12361>
- Shang, Y., You, B., & Shang, L. (2016). China's environmental strategy towards reducing deep groundwater exploitation. *Environmental Earth Sciences*, 75, 1439. <https://doi.org/10.1007/s12665-016-6110-7>
- She, D., Xia, J., Shao, Q., Taylor, J. A., Zhang, L., Zhang, X., Zhang, Y., & Gu, H. (2017). Advanced investigation on the change in the streamflow into the water source of the middle route of China's water diversion project. *Journal of Geophysical Research*, 122(13), 6950–6961. <https://doi.org/10.1002/2016JD025702>
- Song, X., Zhuang, Y., Wang, X., & Li, E. (2018). Combined effect of Danjiangkou reservoir and cascade reservoirs on hydrologic regime downstream. *Journal of Hydrologic Engineering*, 23(6), 05018008. [https://doi.org/10.1061/\(ASCE\)HE.1943-5584.0001660](https://doi.org/10.1061/(ASCE)HE.1943-5584.0001660)
- Stone, R., & Jia, H. (2006). Going against the flow. *Science*, 313, 1034–1037. <https://doi.org/10.1126/science.313.5790.1034>
- Sun, Y., Tian, F., Yang, L., & Hu, H. (2014). Exploring the spatial variability of contributions from climate variation and change in catchment properties to streamflow decrease in a mesoscale basin by three different methods. *Journal of Hydrology*, 508(2014), 170–180. <https://doi.org/10.1016/j.jhydrol.2013.11.004>
- Wada, Y., Lo, M., Yeh, P. J.-F., Reager, J. T., Famiglietti, J. S., Wu, R., & Tseng, Y. (2016). Fate of water pumped from underground and contributions to sea-level rise. *Nature*, 6(8), 777–780. <https://doi.org/10.1038/nclimate3001>
- Wang, S., Li, J., Liu, Y., Liu, J., & Wang, X. (2019). Impact of South-to-North water diversion on groundwater recovery in Beijing [in Chinese]. *China Water Resources*, 26–29.
- Wang, Y., Guo, S., Yang, G., Hong, X., & Hu, T. (2014). Optimal early refill rules for Danjiangkou Reservoir. *Water Science and Engineering*, 16(4), 403–419. <https://doi.org/10.3882/j.issn.1674-2370.2014.04.006>
- Wang, Y., Wang, D., & Wu, J. (2015). Assessing the impact of Danjiangkou reservoir on ecohydrological conditions in Hanjiang river, China. *Ecological Engineering*, 81, 41–52. <https://doi.org/10.1016/j.ecoleng.2015.04.006>
- Wang, Y., Zhang, W., Zhao, Y., Peng, H., & Shi, Y. (2016). Modelling water quality and quantity with the influence of inter-basin water diversion projects and cascade reservoirs in the Middle-lower Hanjiang River. *Journal of Hydrology*, 541, 1348–1362. <https://doi.org/10.1016/j.jhydrol.2016.08.039>
- Xia, J., Wang, Q., Zhang, X., Wang, R., & She, D. (2018). Assessing the influence of climate change and inter-basin water diversion on Haihe River basin, eastern China: a coupled model approach. *Hydrogeology Journal*, 26(5), 1455–1473. <https://doi.org/10.1007/s10040-018-1773-7>

- Xu, Y., & Chang, F. (2009). Preliminary study on requirement rate of ecological water demand in middle and lower reaches of Hanjiang River [in Chinese]. *Journal of Yangtze River Scientific Research Institute*, 26(1). 1–4.
- Yang, G., Guo, S., Li, L., Hong, X., & Wang, L. (2016). Multi-objective operating rules for Danjiangkou reservoir under climate change. *Water Resources Management*, 30(3), 1183–1202. <https://doi.org/10.1007/s11269-015-1220-7>
- Yang, G., Guo, S., Liu, P., Li, L., & Xu, C. (2017). Multiobjective reservoir operating rules based on cascade reservoir input variable selection method. *Water Resources Research*, 53, 3446–3463. <https://doi.org/10.1002/2016WR020301>
- Yang, J., Zhao, H., Yang, Z., Huang, Z., Bai, G., & Liu, C. (2018). The strategy of reducing groundwater exploitation and the south-to-north water diversion project. *International Journal of Environmental Studies*, 57, 59–67. <https://doi.org/10.1080/00207233.2017.1389569>
- Yang, Y., Li, G., Dong, Y., Li, M., Yang, J., Zhou, D., & Zheng, F. (2012). Influence of South to North Water Transfer on groundwater dynamic change in Beijing Plain. *Environmental Earth Sciences*, 65, 1323–1331. <https://doi.org/10.1007/s12665-011-1381-5>
- Yangtze River Water Conservancy Commission (YRWCC) (2018). Annual Bulletin of Water Resources in Yangtze River Basin. [Available at: <http://www.cjw.gov.cn/>]
- Ye, A., Duan, Q., Chu, W., Xu, J., & Mao, Y. (2014). The impact of the South-North Water Transfer Project (CTP)'s central route on groundwater table in the Hai River basin, North China. *Hydrological Processes*, 28(23), 5755–5768. <https://doi.org/10.1002/hyp.10081>
- Zhang, M., Hu, L., Yao, L., & Yin, W. (2018). Numerical studies on the influences of the South-to-North Water Transfer Project on groundwater level changes in the Beijing Plain, China. *Hydrological Processes*, 32, 1858–1873. <https://doi.org/10.1002/hyp.13125>
- Zhang, Z., Fei, Y., Chen, Z., et al. (2009). Survey and Evaluation of Ground-Water Sustainable Utilization in North China Plain [in Chinese]. Geological House, Beijing.
- Zhou, Y., & Guo, S. (2013). Incorporating ecological requirement into multipurpose reservoir operating rule curves for adaptation to climate change. *Journal of Hydrology*, 498, 153–164. <https://doi.org/10.1016/j.jhydrol.2013.06.028>

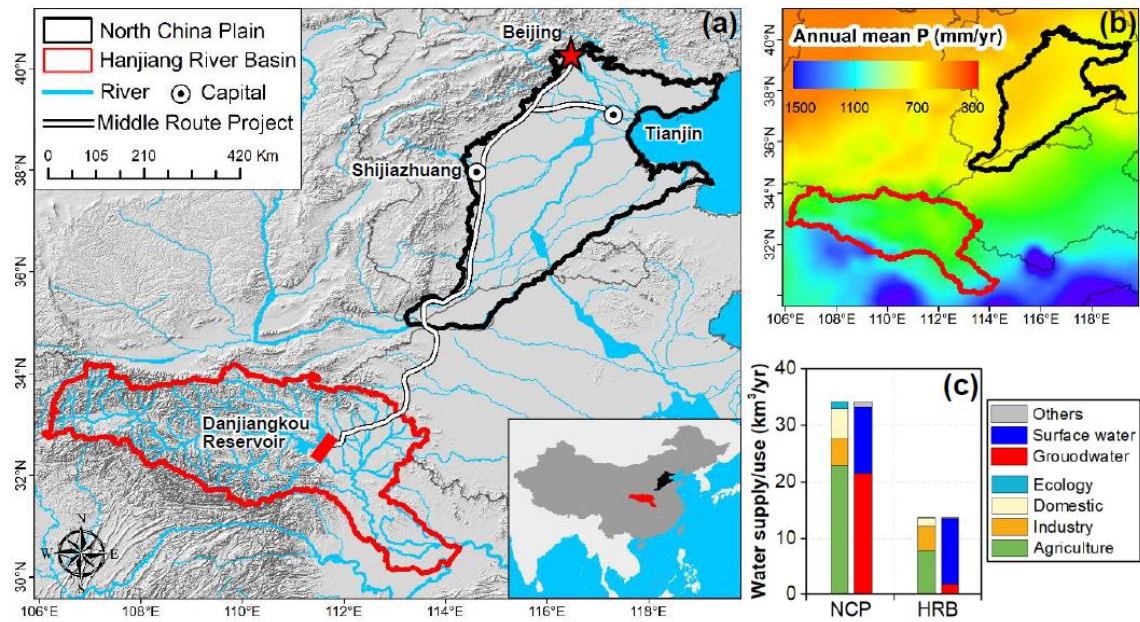


Figure 1. (a) Locations of North China Plain (NCP, ~140,000 km²) and Hanjiang River Basin (HRB, ~159,000 km²) connected by the South-to-North Water Diversion Middle Route Project. (b) The spatial distribution of annual mean precipitation. (c) Histogram of the human water supply by groundwater, surface water and other recycled water, as well as the human water use by four sectors of agriculture, industry, domestic and ecology in two regions. The data are collected from the official water resources bulletins (HRWCC, 2018; YRWCC, 2018).

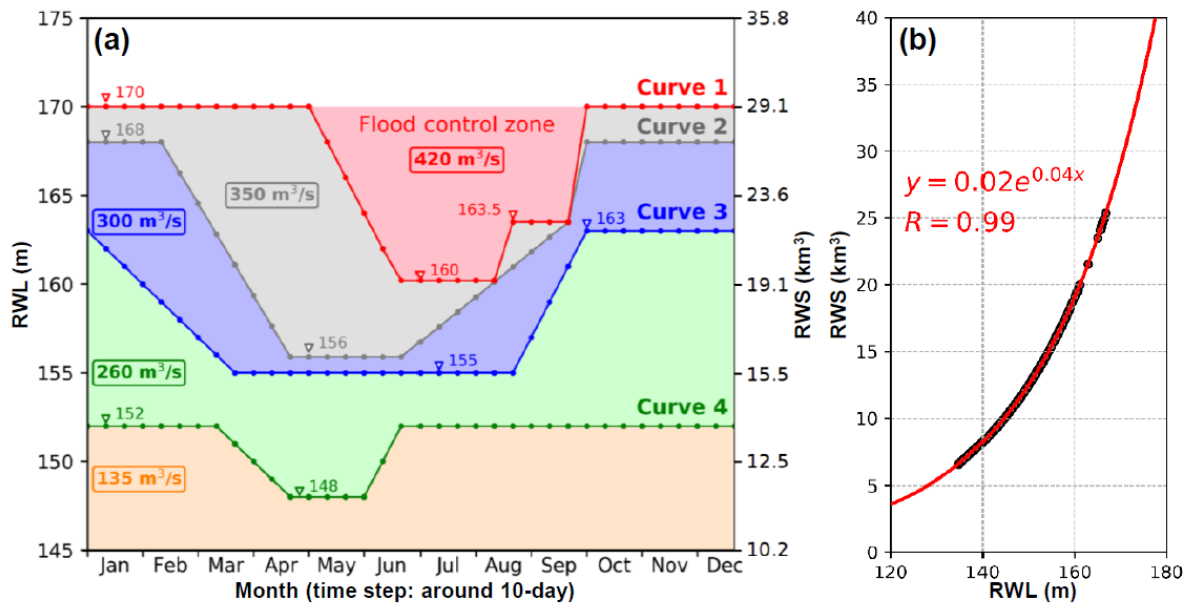


Figure 2. (a) Schematic diagram in the operational rules of DR. Five water diversion rates (i.e., 420, 350, 300, 260 and 135 m³/s) are regulated by four different water level heights from Curve-1 to Curve-4. Since the DR operation interval is ~10-day, each month of a year is divided into three periods. (b) The observed and fitted rating curve of DR (i.e., relation between RWL and RWS), with the fitting formula and correlation coefficient (R) given accordingly. The data of RWL and RWS are collected from the official reservoir management system of the Hydrological Bureau in Hubei province (<http://113.57.190.228:8001/web/Report/BigMSKReport#>)

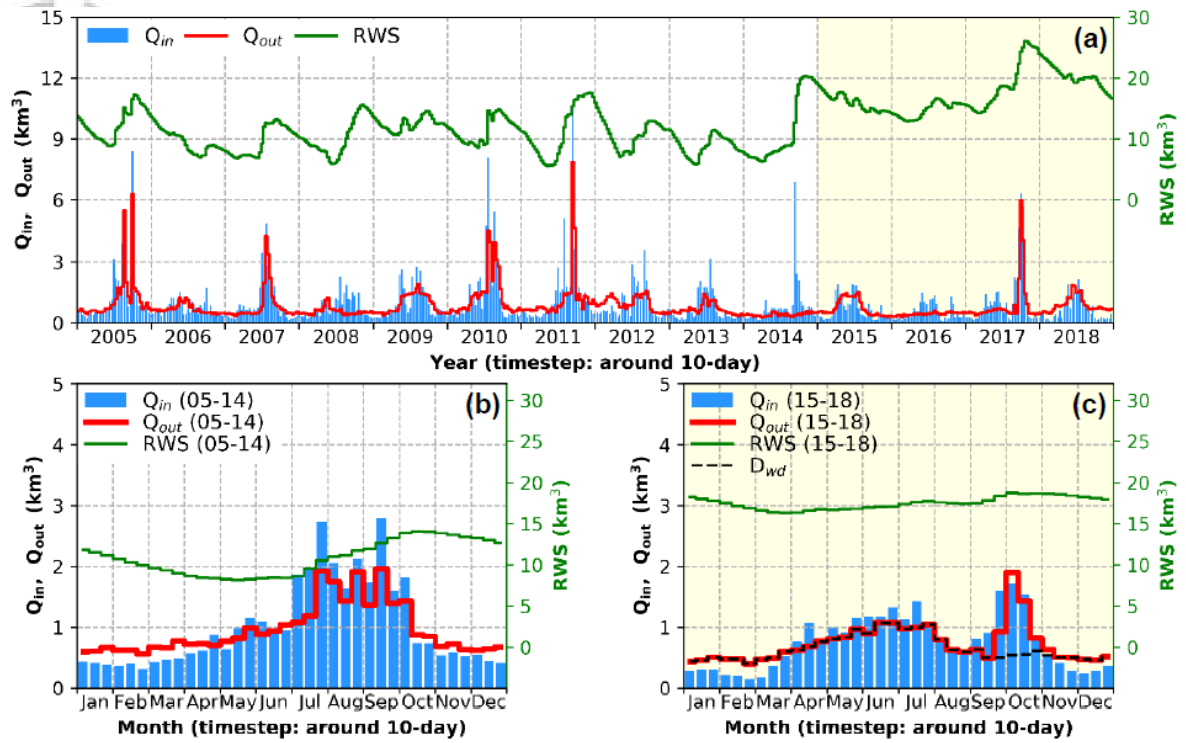


Figure 3. (a) The 2005-2018 10-day aggregated time series of Q_{in} , Q_{out} , and RWS of DR, and the (b) 2005-2014 and (c) 2015-2018 piecewise mean annual cycles of Q_{in} , Q_{out} , and RWS of DR. Note that in Figure 3c the estimate of D_{wd} is the same as Q_{out} except without considering the high flood discharge of Q_{out} in late 2017.

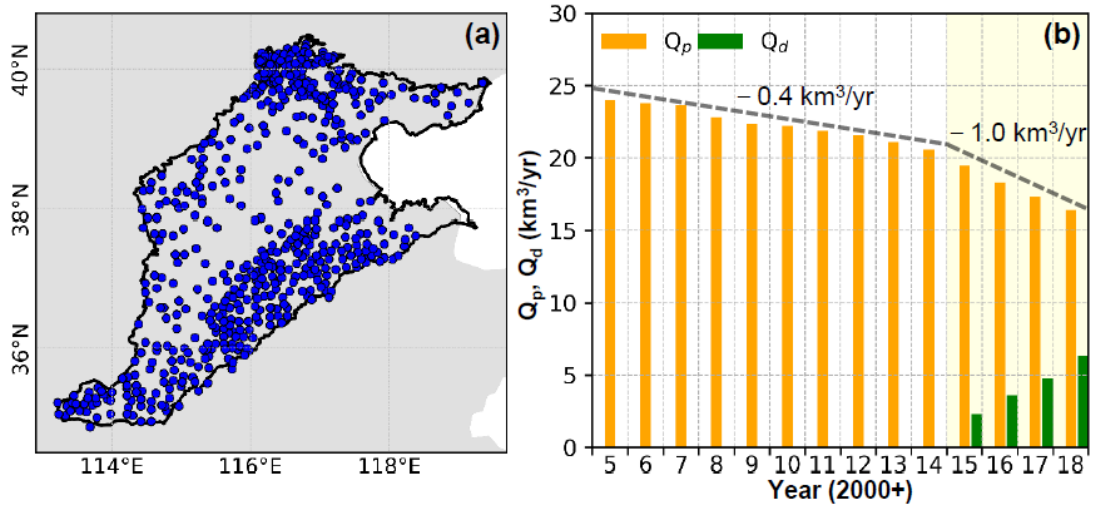


Figure 4. (a) Spatial distribution of groundwater monitoring well locations, and (b) annual times series of Q_p and Q_d during 2005-2018 and 2015-2018, respectively.

Accepted

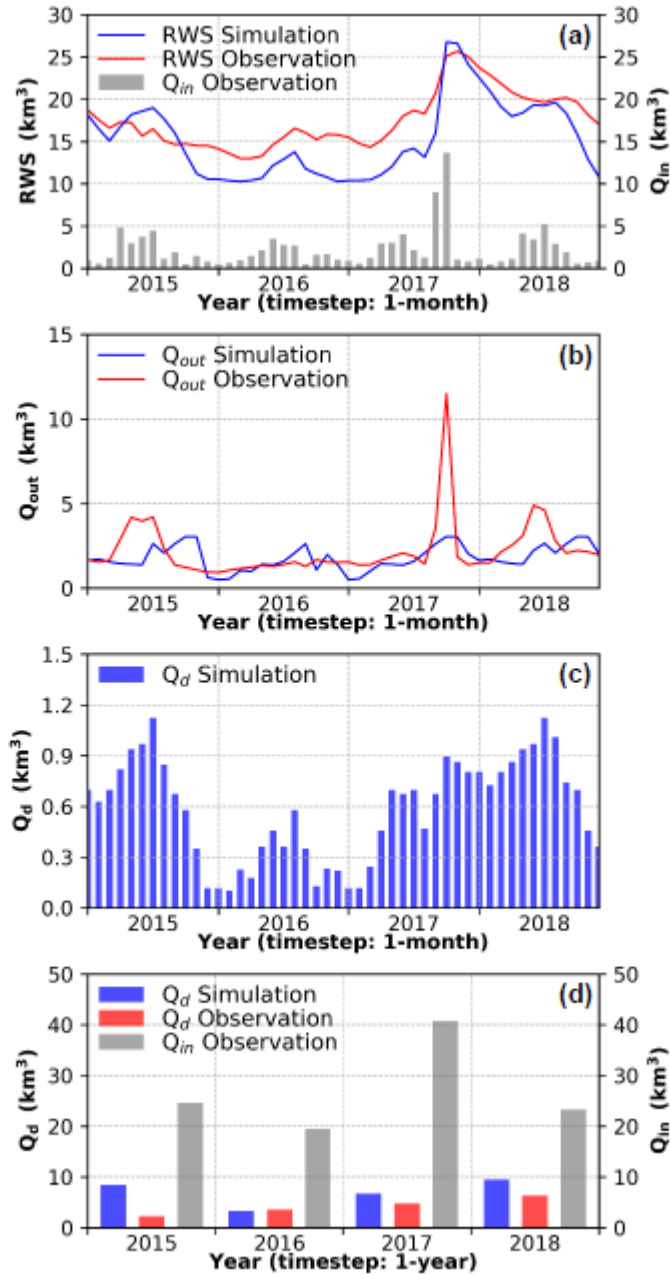


Figure 5. The 2015-2018 monthly and annual time series of DR water budget components from the actual observation and the water diversion simulation with $D_{wd}=23.2 \text{ km}^3/\text{yr}$. (a) Monthly RWS and Q_{in} ; (b) monthly Q_{out} ; (c) monthly Q_d ; and (d) annual Q_d and Q_{in} .

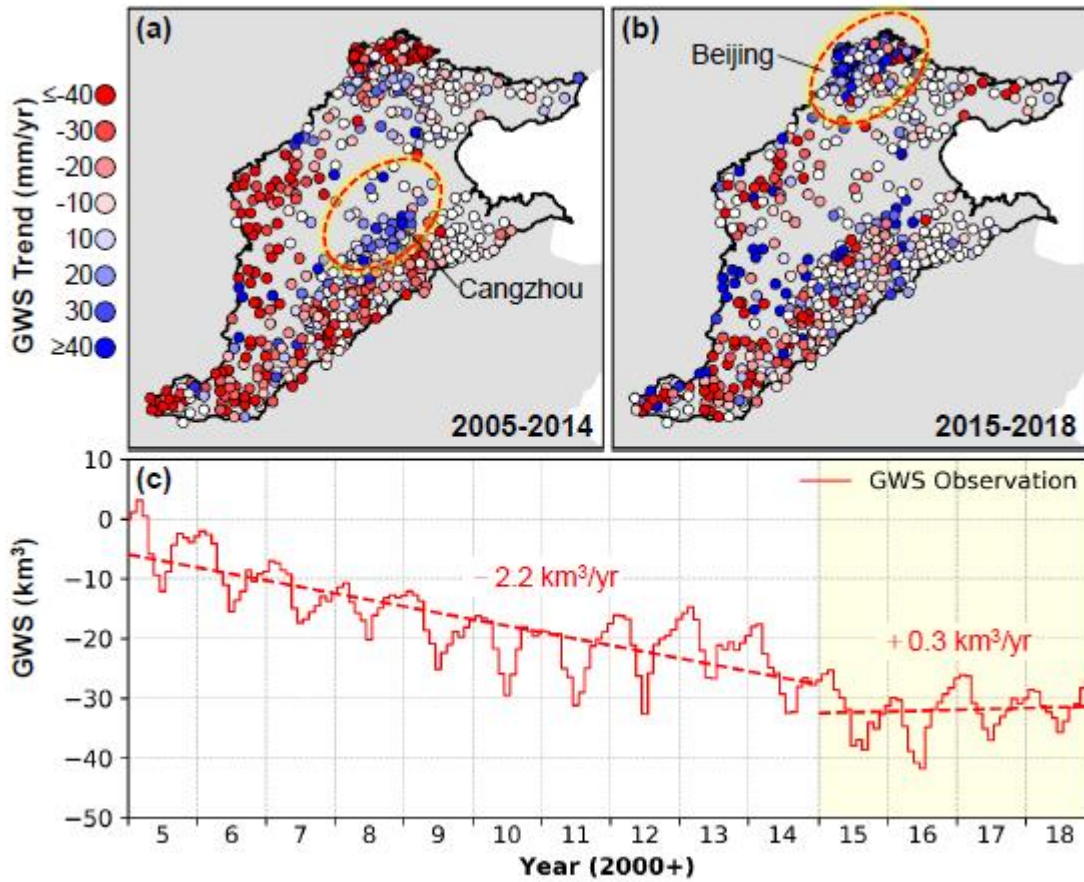


Figure 6. Spatial distribution maps of GWS trends observed by 559 unconfined wells during (a) 2005-2014 and (b) 2015-2018, as well as (c) the corresponding 2005-2018 monthly time series of GWS variations in NCP.

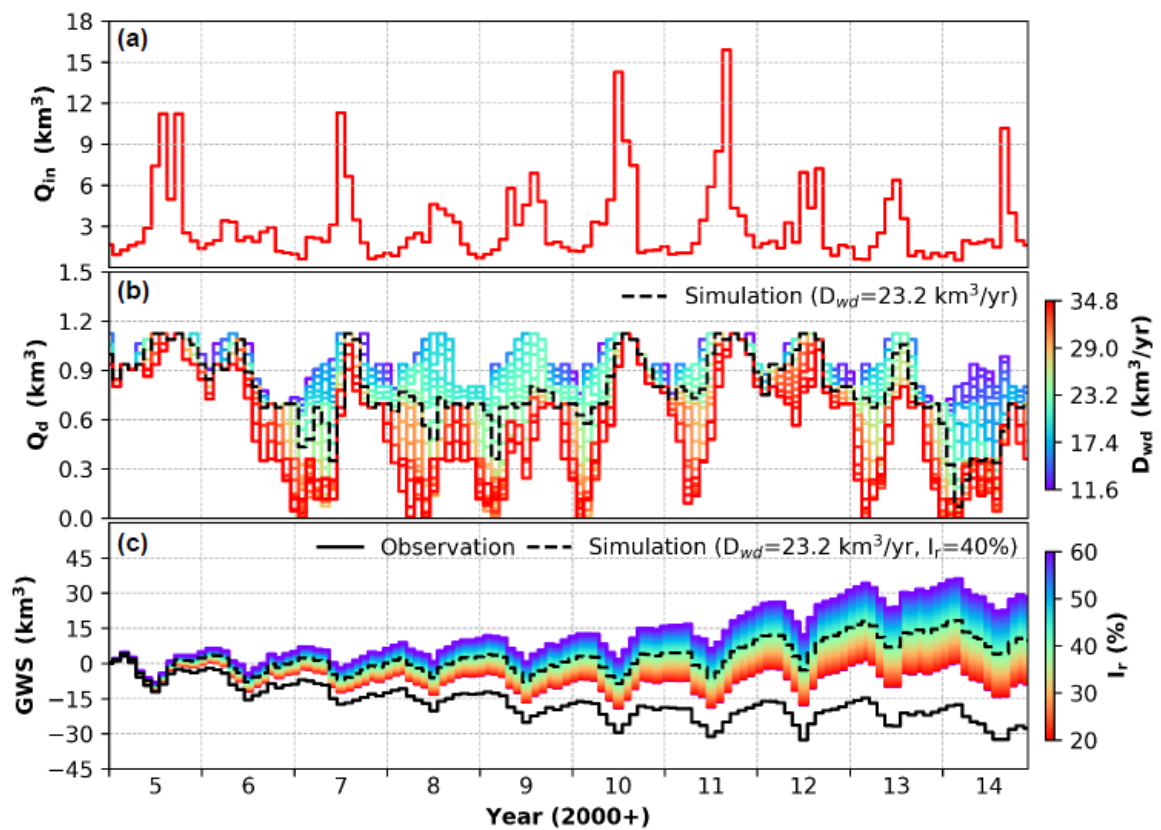


Figure 7. The 2005-2014 monthly time series of the observed (a) Q_{in} and the simulated (b) Q_d in DR with varying D_{wd} between 11.6~34.8 km³/yr. (c) The 2005-2014 monthly time series of the observed GWS and the simulated GWS in NCP after receiving the simulated Q_d ($D_{wd}=23.2$ km³/yr) with varying I_r between 20~60%.

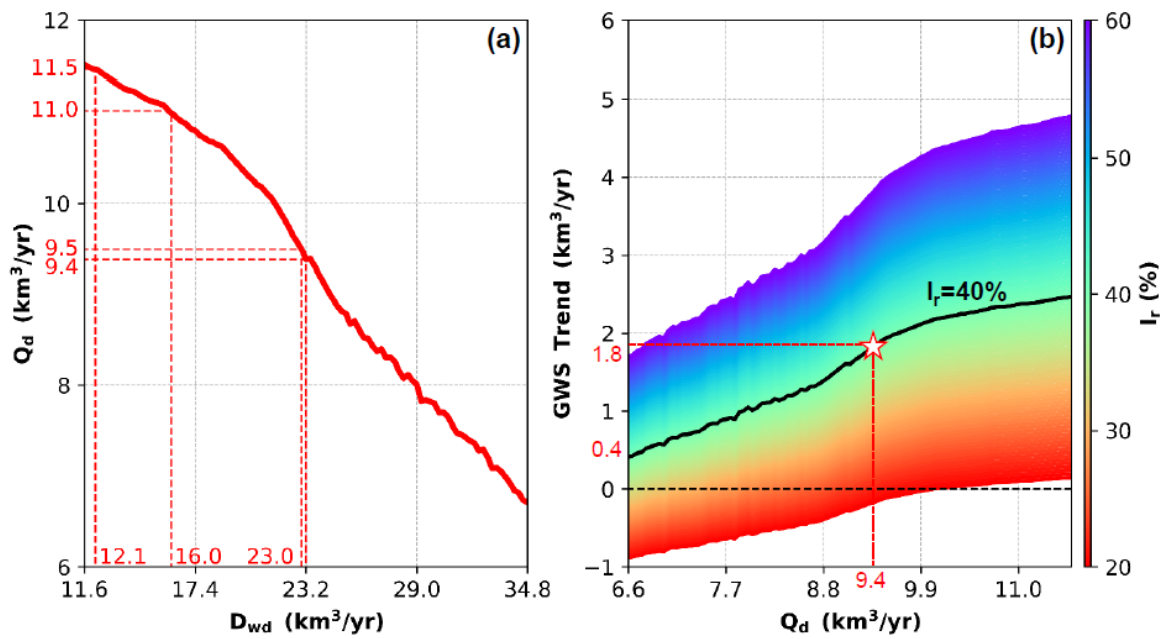


Figure 8. (a) Changes of the 2005-2014 mean annual Q_d ($6.6\sim 11.6 \text{ km}^3/\text{yr}$) with varying D_{wd} ($11.6\sim 34.8 \text{ km}^3/\text{yr}$) in ensemble water diversion simulations, and (b) the corresponding changes of the 2005-2014 annual GWS trends after receiving the simulated Q_d with varying I_r ($20\sim 60\%$) in NCP.